Available online at www.sciencedirect.com

jmr&t Journal of Materials Research and Technology

www.jmrt.com.br

Original Article

Photocatalytic performance of N-doped TiO_2nano-SiO_2-HY nanocomposites immobilized over cotton fabrics

Salmon Landi Jr.[a,b,*], *Joaquim Carneiro*[a], *Olivia S.G.P. Soares*[c], *Manuel F.R. Pereira*[c], *Andreia C. Gomes*[d], *Artur Ribeiro*[e], *António M. Fonseca*[e,f], *Pier Parpot*[e,f], *Isabel C. Neves*[e,f]

[a] *Department of Physics, University of Minho, Azurém Campus, Guimarães 4800-058, Portugal*
[b] *Instituto Federal Goiano, 75901-970 Rio Verde, Goiás, Brazil*
[c] *Laboratory of Catalysis and Materials – Associate Laboratory LSRE/LCM, Faculty of Engineering, University of Porto, 4200-465 Porto, Portugal*
[d] *Centre of Molecular and Environmental Biology, University of Minho, 4710 – 057 Braga, Portugal*
[e] *Centre of Biological Engineering, University of Minho, 4710-057 Braga, Portugal*
[f] *Centre of Chemistry, Chemistry Department, University of Minho, Gualtar Campus, Braga 4710-057, Portugal*

ARTICLE INFO

Article history:
Received 15 January 2018
Accepted 4 June 2018
Available online 23 February 2019

Keywords:
Photocatalysis
Textile functionalization
TiO_2-SiO_2
HY zeolite
Rhodamine B
Cytotoxic

ABSTRACT

This work reports the synthesis of nanocomposite photocatalytic materials based on nitrogen-doped TiO_2nano, SiO_2 and different percentages of HY zeolite (0, 12, 25 and 50%). These materials were characterized by using Fourier transformed infrared spectroscopy, X-ray diffraction, N_2 adsorption–desorption, UV-vis diffuse reflectance spectroscopy and scanning electron microscopy. The nanocomposites, which presented an energy band gap of about 3.03 eV, were immobilized on cotton fabric and their self-cleaning properties were investigated by decolourization of rhodamine B (RhB) dye in aqueous solution under simulated solar irradiation. The fabrics coated with the photocatalysts, containing and not containing zeolites, showed the same RhB decolourization (about 95%) after 5 h, excluding the situation where a large amount of HY (50%) was used in the nanocomposites. However, results obtained from high performance liquid chromatography analysis depicted that in the presence of the HY zeolite a more effective RhB degradation was achieved. In fact, even after the use of five consecutive cycles, the RhB decolourization remained high (about 85%). Generally, the photodegradation of RhB solution in the presence of cotton fabrics functionalized with TiO_2nano, TiO_2nano-SiO_2 and TiO_2nano-SiO_2-0.25 HY resulted in the formation of products that exhibited a similar cytotoxic effect when compared to the untreated RhB solution and subjected to the same tested concentrations and incubation times.

Published by Elsevier Editora Ltda. on behalf of Brazilian Metallurgical, Materials and Mining Association. This is an open access article under the CC BY-NC-ND license (http://creativecommons.org/licenses/by-nc-nd/4.0/).

* *Corresponding author.*
E-mail: salmon.landi@ifgoiano.edu.br (S. Landi Jr.).
https://doi.org/10.1016/j.jmrt.2018.06.025
2238-7854/Published by Elsevier Editora Ltda. on behalf of Brazilian Metallurgical, Materials and Mining Association. This is an open access article under the CC BY-NC-ND license (http://creativecommons.org/licenses/by-nc-nd/4.0/).

1. Introduction

Several works have been reported in the literature on heterogeneous photocatalysis, which usually explores the degradation of pollutants by redox reactions that begins near the surface of semiconductors after being subjected to light irradiation [1]. Due to its electronic structure, characterized by the presence of a nearly filled valence band (VB) and an practically empty conduction band (CB) separated by a band gap energy (E_g), the semiconductors can absorb photons whose energy is equal to or greater than E_g and as a consequence, electron–hole (e^-/h^+) pairs are generated. The charge carriers which did not undergo the recombination process can react with electron donors (e.g. H_2O or pollutant) or electron acceptors (e.g. O_2) adsorbed on the semiconductor surface creating free radicals [2]. These species are highly reactive leading to the degradation of different pollutants, such as pesticides [3], pharmaceuticals [4], dyes [5], gases [6], or removing toxic heavy metal, such as Hg^0 from flue gas [7] or even inactivating microorganisms (virus, bacteria, spores and protozoa) [8]. It is important to note that according to Derikvandi and Nezamzadeh-Ejhieh the major limitation of heterogeneous photocatalysis is the recombination of e^-/h^+ pairs, and that this problem can be relatively mitigated by doping, supporting and coupling of semiconductors [9].

Particularly, the dyes from the textile industries represent an important class of pollutants because of their huge world production (about 10^5 tonnes/year [10]) and due to its frequent discharge in water courses [11]. It is estimated that about 15% of the dyes are lost in the industrial effluents during manufacturing process [12]. In addition, some dyes are non-biodegradable and other can be metabolized into carcinogenic by-products [13]. Since the conventional methods used in the wastewater treatments, such as flocculation, chemical precipitation and adsorption on activated carbon do not promote the degradation of these pollutants, but only transfer them to other media (causing secondary pollution) [14], the photocatalysis enabled by semiconductor materials has been considered an efficient technology for remediation of wastewater [15].

Among diverse semiconductors, titanium dioxide (TiO_2) is widely used in photocatalytic reactions and it is also considered as a potential candidate in industrial applications for remediation applications because it is biologically and chemically inert, inexpensive, harmless and non-toxic [10]. However, according to Nezamzadeh-Ejhieh TiO_2 presents low surface area, rapid recombination of e^-/h^+ pairs and in order to be light activated, TiO_2 requires the absorption of photons with energy in the ultraviolet (UV) region due to its large value of band gap energy [16]. Therefore, to better exploit the solar radiation that reaches Earth's surface (UV, 1–380 nm, 5%; visible, 380–780 nm, 46%; near infrared, 780–3000 nm, 49% [17]), researchers have tried to implement different strategies. Among them, the doping process has been applied because it is capable to generate new energy levels inserted between the original VB and CB [18] and also to decrease the recombination process already mentioned [19]. Another strategy concerns the production of hybrid systems with noble metals, which can absorb the visible light by surface plasmon resonance phenomena. This absorbed energy can then be transferred to the CB by charge transfer, promoting, subsequently, the occurrence of reduction reactions [17].

Since the effectiveness of the photocatalysis process is highly dependent upon the charge transfer between the semiconductor and the dissolved species, it is strongly desirable to use materials that are characterized by having a large surface area and acting as dispersive support of the photocatalysts. In this sense, it has been reported that the supporting TiO_2 on activated carbon [20], graphene-based materials [21], SiO_2 [22] can improve the photocatalytic activity of TiO_2 semiconductor material. Currently, zeolites are also widely exploited in the preparation of composites having photocatalytic properties [23–28]. The properties of the zeolites that are interesting for the photocatalysis reactions, mainly include a high internal surface area formed by cannels or cavities and also the presence of ions and acid sites [29]. In fact, in a recent published article, we have shown the potential use of the HY zeolite in promoting the photocatalytic activity of cotton textiles functionalized with SiO_2-TiO_2 and SiO_2-TiO_2-HY composites [30]. In that work, several experimental parameters were evaluated and the best catalytic performance was achieved for the SiO_2-TiO_2 and SiO_2-TiO_2-HY composites that were subjected to a calcination treatment at a temperature of 400 °C.

However, for a scenario of industrial applications, there are some drawbacks related with the use of the photocatalysts in the form of directly added powder to promote the remediation of wastewater. For example, powders present a tendency to form agglomerates and, as consequence, they can precipitate, thus decreasing the material availability to participate into photodegradation reactions. Therefore, unless some kind of stirring system is used, which can undoubtedly lead to increased energy consumption, the direct addition of photocatalyst powder should be avoided. Other inconvenient is related to the photocatalyst reuse, since the separation of powders from treated effluents will certainly increase the treatment costs. Therefore, the photocatalysts impregnation on a solid support can be an important and smart alternative to overcome the previous mentioned difficulties [31]. Moreover, several works have also chosen textile materials to obtain self-cleaning photocatalytic surfaces because they are cheap, present low weight and high mechanical flexibility and, in addition, they can also be easily adjusted to the different geometries of treatment tanks that would have already been installed in the original industrial layouts. Recently, Fan et al. demonstrated a remarkable photocatalytic activity and removal of stains using g-C3N4 onto cotton fabrics under sunlight irradiation [32]. El-Naggar et al. synthetized SiO_2-ZnO nanocomposites over cotton fabrics with antibacterial and UV protection properties [33]. Similar materials were obtained by Mehrez et al. from in situ synthesis of TiO_2 on cotton fabrics using urea nitrate as a peptizing agent [34] and by Mohamed et al. from functionalization of cotton textiles with Ag and SiO_2 nanoparticles [35]. Katoueizadeh et al. applied N-doped TiO_2 over cotton textiles to produce samples that presents photocatalytic and super hydrophobic behaviour under visible light irradiation [36]. In order to follow up on our previous work, a photocatalytic composite based on the TiO_2 nanoparticles, SiO_2, and HY zeolite was impregnated on the cotton fabrics and a lamp that simulated the solar radiation was used

to promote the degradation of rhodamine B (RhB), a widely used dye in textile industry effluents [37]. In particular, RhB ($C_{28}H_{31}N_2O_3Cl$) is a dye of the xanthene class that causes irritation to the skin, eyes and respiratory tract and even possess carcinogenicity, reproductive and progressive toxicity [37].

2. Experimental

2.1. Materials

Tetraethoxysilane (TEOS) was used as precursor for SiO_2 and purchased from Aldrich. The HY zeolite (CBV 400) was obtained from Zeolyst International in powdered form. Commercial TiO_2 nanoparticles were acquired from Quimidroga and consisted in a mixture of anatase (80%) and rutile (20%) crystalline phases. Ethanol and water were used as solvents and ammonium hydroxide was utilized as a catalyst for hydrolysis reactions.

2.2. Preparation and characterization of composites and self-cleaning fabrics

The photocatalysts preparation method was similar to the one described in our previous and recent published work [30]. Typically, the hydrolysis of the SiO_2 precursor (2.30 g) was achieved in the presence of TiO_2 nanoparticles (1.44 g), ethanol (1.20 mL) and H_2O (1.00 mL) in alkaline media. However, in this work a substantial amount (0.5 mL) of ammonium hydroxide (NH_4OH) was used in order to obtain nitrogen-doped TiO_2 nanoparticles. Hereafter, the HY zeolite was added in the refluxed solution, which was magnetically stirred for 6 h and finally dried at 70 °C in an oven. Different amounts of zeolite (0, 12, 25 and 50% taken in relation to the sum of the weights of SiO_2 precursor and TiO_2 nanoparticles) were employed. The nanocomposites containing an increasing amount of the HY zeolite were denoted as TiO_2nano-SiO_2, TiO_2nano-SiO_2-0.12HY, TiO_2nano-SiO_2-0.25HY and TiO_2nano- SiO_2-0.50HY and their properties were compared to bare TiO_2. Since the TiO_2 nanoparticles present crystalline phases and the zeolite is already acidic, the calcination step was not performed in this work [30].

The photocatalyst nanocomposites were characterized by different techniques. Fourier transform infrared (FTIR) spectra of the nanocomposites in KBr pellets were performed to investigate the vibrations bands on a Bomem MB104 spectrophotometer (range: 4000–500 cm^{-1}, resolution: 4 cm^{-1} using 32 scans). The powder X-ray diffraction (XRD) was performed to analyze the crystal structure of the nanocomposites on a Bruker D8 Discover (scan range: 5–60° at a scan rate of 0.1°/s). The textural properties of the nanocomposites were determined by adsorption–desorption of N_2 at −196 °C on a Nova 4200e (Quantachrome Instruments) equipment. The micropores volumes (V_{micro}) and mesoporous surface areas (S_{meso}) were calculated by using the *t*-method, the BET surface areas (S_{BET}) were determined via BET equation and the total pore volume was obtained for $P/P_0 = 0.95$ (V_P). Transformed Kubelka–Munk function, obtained from the ultraviolet-visible diffuse reflectance spectra (UV-vis DRS) acquired on a ScanSpecUV-vis spectrophotometer equipped with an integrating sphere, was used to calculate the band gap energy (E_g) of the as-prepared photocatalyst nanocomposites.

The functionalization of the cotton fabrics (3 cm × 3 cm) with the photocatalyst nanocomposites, essentially consisted of the following three steps: (i) initially, a methanol/composite suspension was homogenized by sonication during 15 min; (ii) the cotton fabrics were dipped in the suspension and stayed there for 15 min under sonication and (iii) after that time, the sonicator was switched off but the cotton fabrics still remained in the suspension during 1 min and then removed to let them to dry at room temperature. Actually, step (ii) consists of an important modification to the methodology performed by Xu et al. [38] because it enables a better interaction between the cotton fibres and the nanocomposite particles, thus improving the fabrics functionalization process. The step (iii) was repeated two times in the same suspension and, finally, the samples were cured in an oven at 100 °C for 10 min. The micrographs of the nanocomposites and the self-cleaning fabrics were examined by scanning electron microscopy (SEM) using a FEI Nova 200 FEG-SEM microscope at a magnification of 5000× and 50,000×.

2.3. Photocatalytic activity

The photocatalytic performance of the different samples was evaluated by the degradation of RhB aqueous solutions (5 mg/L) under similar sunlight irradiation. The experiments were conducted in beakers with 20 mL of dye aqueous solution together with the cotton samples. The beakers were sealed with flexible film (at least having 90% of transmittance in range 300–800 nm) to avoid the evaporation of the solution and then placed in a region, delimited by a circular mark, and whose centre was directly exposed to the light emitted by a 300 W lamp (Ultra-Vitalux E27) and placed at a distance of about 30 cm above the solution surface. The UVA/B and visible light irradiance was around 1.0 and 2.0 mW/cm^2, respectively. The solutions were not subjected to any type of stirring process. In order to distinguish the adsorption and the photocatalytic degradation process, the cotton samples remained in the solutions during 1 h in the dark and, after that time, the lamp (simulating the sunlight spectrum) has been switched on for 5 h. The recyclability of the performance of the cotton fabrics coated with TiO_2nano, TiO_2nano-SiO_2 and TiO_2nano-SiO_2-0.25HY composites was analyzed up to five cycles. Experiments were performed in duplicate and the error bars refer to the standard deviations.

2.4. Analytical methods

The photocatalytic degradation of the RhB solutions was monitored by examining its maximum absorbance values acquired at specific intervals of time. For this purpose, the lamp was switched off and dye solution aliquots (3.0 mL) were extracted and centrifuged at 6000 rpm for 10 min to obtain the supernatant. The absorbance of the supernatant was monitored using a spectrophotometer (ScanSpecUV-Vis) in the 300–700 nm wavelength range and its corresponding concentration was determined from the calibration curve. After performing the absorbance measurements, the supernatants

were re-inserted into the beakers and the lamp was switched on again according to Zhang et al. [39].

The N-de-ethylated intermediates from the photodegradation of RhB were identified by electrospray ionization (ESI) mass spectral technique in the positive ion mode and confirmed by high liquid chromatography performance (HPLC) technique on a Thermo Finnigan Lxq equipped with a UV-vis diode array detector in series with a mass detector using a C18 reverse phase column. The mobile phase consisted in a mixture of an acetic acid solution (0.2%) and acetonitrile at a flow rate of 0.4 mL/min.

2.5. *Cellular viability assay*

2.5.1. *Cell culture maintenance*

NCTC 2544 cell line was used as general model of cytotoxicity. The NCTC 2544 cell line (human skin keratinocytes) was cultured in DMEM media, and supplemented with 7% FBS and 1% (v/v) penicillin/streptomycin solution. Cells were maintained in 75 cm^2 tissue culture flasks at 37 °C in a humidified atmosphere with 5% CO_2. The cell culture medium was renewed twice a week.

2.5.2. *Cell viability assessed by MTT assay*

The MTT (3-(4,5-dimethylthiazol-2-yl)-2,5-diphenyltetrazoliumbromide) assay was used to measure the cytotoxicity of the RhB solutions before and after photocatalytic treatment in cell cultures [40]. Cells were seeded at a previously optimized density of 1×10^5 cells/mL on a 48-well tissue culture plate, the day before the experiments. NCTC 2544 cells were exposed to four concentrations (0.015, 0.025, 0.050 and 0.075 ppm) of RhB solutions obtained before and after photocatalytic treatment. Cells incubated with DMSO (30% of the total volume) and cells without the addition of the compounds were used as positive and negative controls of cytotoxicity, respectively. Cells were incubated at 37 °C in a humidified atmosphere with 5% CO_2. At the end of 24 and 48 h of contact, cell metabolic activity was assessed by MTT viability assay [40]. After incubation, the medium with RhB samples was removed and medium with MTT (5 mg/mL) was added to each well, and cells were further incubated at 37 °C for 2 h. The MTT solution was carefully decanted, and formazan crystals were dissolved in DMSO/EtOH (1:1 (v/v)) mixture. Colour was measured with 96-well plate reader at 570 nm in a microplate reader SpectraMax Plus (Molecular Devices). Cellular viability was determined in relation to the life control from the three independent experiments.

2.5.3. *Statistical analysis*

Data are presented as average standard deviation (SD), $n = 3$. Statistical comparisons were performed by one-way ANOVA with GraphPad Prism 7.0 software (La Jolla, CA, U.S.A.). Tukey's post hoc test was used to compare all the results between them, and a Dunnet's test was used to compare the results with a specific control. A P-value of <0.05 was considered to be statistically significant.

3. Results and discussion

3.1. *Characterization of the photocatalyst nanocomposites*

In this work, the nanocomposites were prepared with TiO_2 nanoparticles and the zeolite HY. This zeolite belongs to faujasite structure [41] and it was used as received in the proton form with a total ratio Si/Al 2.80 and presents a pH value of 4.5 at the point of zero charge (pH_{PZC}), which confirms the acidic behaviour of the structure. The pH_{PZC} of the zeolite was determined by the procedure describe in [42].

FTIR spectra of the nanocomposites show the strong bands attributed to the HY zeolite structure (Fig. S1) [43]. The vibration mode detected between 570 and 600 cm^{-1} is very sensitive to changes in the HY zeolite structure and can be used to calculate the framework Si/Al ratio [30]. This band did not undergo any shift and therefore, all composites showed the same framework Si/Al ratio (2.75) suggesting that the nanocomposite preparation did not change the HY zeolite structure, in agreement to the expected value (2.80). On the other hand, only for the nanocomposite without the presence of HY zeolite, it was possible to identify a band at about 960 cm^{-1} confirming the existence of linkages of Si–O–Ti [38,44]. Probably, in the nanocomposite spectra, there was a superposition of this band with the strong bands of the HY zeolite precluding its identification.

The XRD patterns of the photocatalysts and the HY zeolite are depicted in Fig. S2. The diffraction peaks of the nanocomposites show that the TiO_2 nanoparticles consist in a mixture of anatase (JCPDS, no. 21-1272) and rutile (JCPDS, no. 21-1276) phases and their intensities confirm that anatase is the dominant crystalline phase. The unit cell parameter of the HY zeolite (face centred cubic structure) was determined from the angular positions of the (5 3 3), (6 4 2) and (5 5 5) diffractions peaks by using the ASTM D 3942-80 method. Subsequently, the framework Si/Al ratio of the zeolite HY was determined by using the Breck and Flanigen equation [30]. These three Miller diffraction peaks, which were previously mentioned, presented the same diffraction angles in the diffractograms of the HY zeolite and the nanocomposites, which confirms that there was not dealumination of the zeolite structure during the composites preparation process. The obtained value from the XRD (Si/Al = 2.87) is in good agreement with the expected one.

The nitrogen adsorption–desorption equilibrium isotherms at −196 °C reveal that the presence of the HY zeolite enhances the surface area as well as the total pore volume of the SiO_2-TiO_2-HY composites, which is related to the high surface area of the HY zeolite, as can be observed in Table 1. It can be observed that TiO_2nano-SiO_2 material presents a surface area of 53 m^2/g whereas the TiO_2nano-SiO_2-0.12HY show a surface area of 430 m^2/g, evidencing that even using a small amount of HY zeolite, it significantly enhances the S_{BET}. As expected, the nanocomposite synthesis leads to a decrease of the microporosity comparing to HY, which should be related to the mesoporous nature of the TiO_2nano and TiO_2nano-SiO_2 materials.

Table 1 – Physical properties of the pristine and nanocomposite materials.

Sample	S_{BET} (m^2/g)	S_{meso} (m^2/g)	V_{micro} (cm^3/g)	$V_{P\ P/P0=0.95}$ (cm^3/g)
TiO_2nano	41	41	0.000	0.079
TiO_2nano-SiO_2	53	49	0.001	0.111
HY	665	25	0.302	0.349
TiO_2nano-SiO_2-0.12HY	430	317	0.050	0.386
TiO_2nano-SiO_2-0.50HY	497	263	0.097	0.348

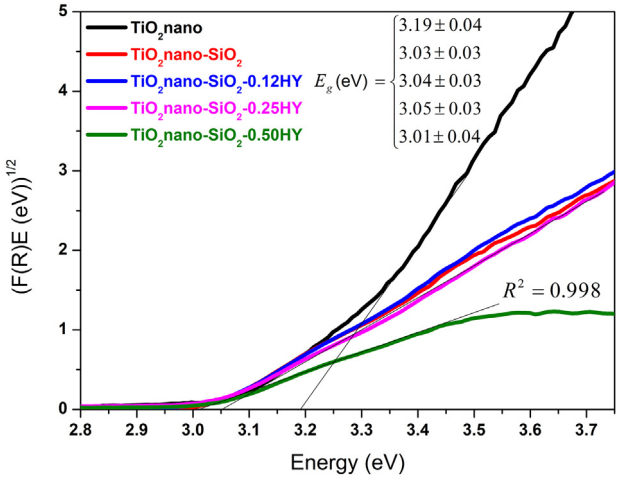

Fig. 1 – Kubelka–Munk transform versus photon energy of the prepared nanocomposites compared to TiO_2 nanoparticles.

DRS were thoroughly investigated such that all the conditions required by the Kubelka–Munk theory were satisfied. From the reflectance (R_∞) measurements as a function of wavelength of the incident photon the E_g value of the nanocomposites, for indirect optical transitions can be determined by using the equation: $[F(R_\infty)]^{1/2} = C(E - E_g)$ [45,46]. In this equation, the variables, F, E and C are Kubelka–Munk function, incident photon energy and proportionality constant, respectively, which depends on the material properties. The usual procedure consists in plotting the left side of the previous equation against the E variable (that is, the energy of the incident photon) fitting the linear portion of this curve by a straight line (Fig. 1). Therefore, the linear coefficient divided by the slope (taken in module) provides the numerical value of E_g. Fig. 1 shows the determined E_g value of the nanocomposites, which is compared with the E_g value of TiO_2 nanoparticles.

The E_g of TiO_2 nanoparticles was determined to be 3.19 eV, which is a value in accordance to the literature [47]. On the other hand, considering the uncertainties (calculated from the linear fit parameters), all nanocomposites presented the same E_g, which is substantially lower than that of TiO_2. The reason for this E_g decrease probably results from the effect of N-doping of TiO_2 nanoparticles occurred during the preparation method of the nanocomposites. In addition, besides extending the light absorption range (for longer wavelengths) of TiO_2 nanoparticles, the N-doping effect also leads to less a recombination rate of electron–hole pairs, thus enhancing the photocatalytic activity of these photocatalysts [48]. Fig. 1 also shows the R^2 (0.998) obtained from the linear fit as previously explained, showing an excellent linearity, which confirms the consistency of the obtained optical properties for these nanocomposites.

Fig. 2(a)–(c) shows the SEM micrographs of the TiO_2nano, TiO_2nano-SiO_2 and TiO_2nano-SiO_2-0.25HY photocatalysts on the fabric's surface. It is noted that these three photocatalysts are differently dispersed on the cotton substrate. TiO_2 nanoparticles coated better the cotton fibres (Fig. 2(a)) in comparison with the other nanocomposites. In particular, those ones that include the HY zeolite in their compositions tend to form bigger agglomerates (Fig. 2(c)), which is due to the tendency of the zeolite particles to agglomerate and therefore affecting the corresponding catalytic properties.

Fig. 2(d) and (e) shows the morphology of TiO_2 nanoparticles and TiO_2nano-SiO_2-0.25HY nanocomposite, respectively, at a magnification of 50,000×. The histogram (Fig. S3) represents the size distribution of TiO_2 nanoparticles and it was obtained from analysis of Fig. 2(d) and the respective average particle size was found to be 40 ± 7 nm. This value is much higher than that of the pore diameter of HY zeolite (0.74 nm), thus these TiO_2 nanoparticles can be only impregnated onto the surface of the zeolite particles, as is shown in the Fig. 2(e). Fig. 2(f) depicts the EDX results from the square region highlighted in the Fig. 2(e). Although only TiO_2 nanoparticles are visible in this highlighted region (Fig. 2(e)), the presence of the zeolite and the SiO_2 is confirmed through the quantification of Si and Al atoms in the EDX analysis. This confirms that for the nanocomposites based in TiO_2, SiO_2 and HY zeolite, the TiO_2 nanoparticles are impregnated at surface of the zeolite particles.

The essential idea of this work consists in proving that the photodegraded products near to TiO_2 surface can be better degraded by the action of the acid sites present in the HY zeolite, whereas the role of SiO_2 is to act as a bond between these two different materials.

3.2. *Photocatalytic degradation of RhB dye*

The photocatalytic ability of the fabrics was evaluated by decolourization of RhB solution calculated by equation: $\text{Decolourization}\,(\%) = (1 - C/C_0) \times 100$ The RhB concentration also was analyzed from the pseudo-first-order kinetic model: $\ln(C/C_0) = -k_{app}t$. In these equations, C_0 is the RhB dye concentration after its adsorption during 1 h in dark conditions, C represents its concentration after being subjected to irradiation of light performed at different interval of times (t) and k_{app} is the pseudo-first-order kinetic reaction constant [49]. As

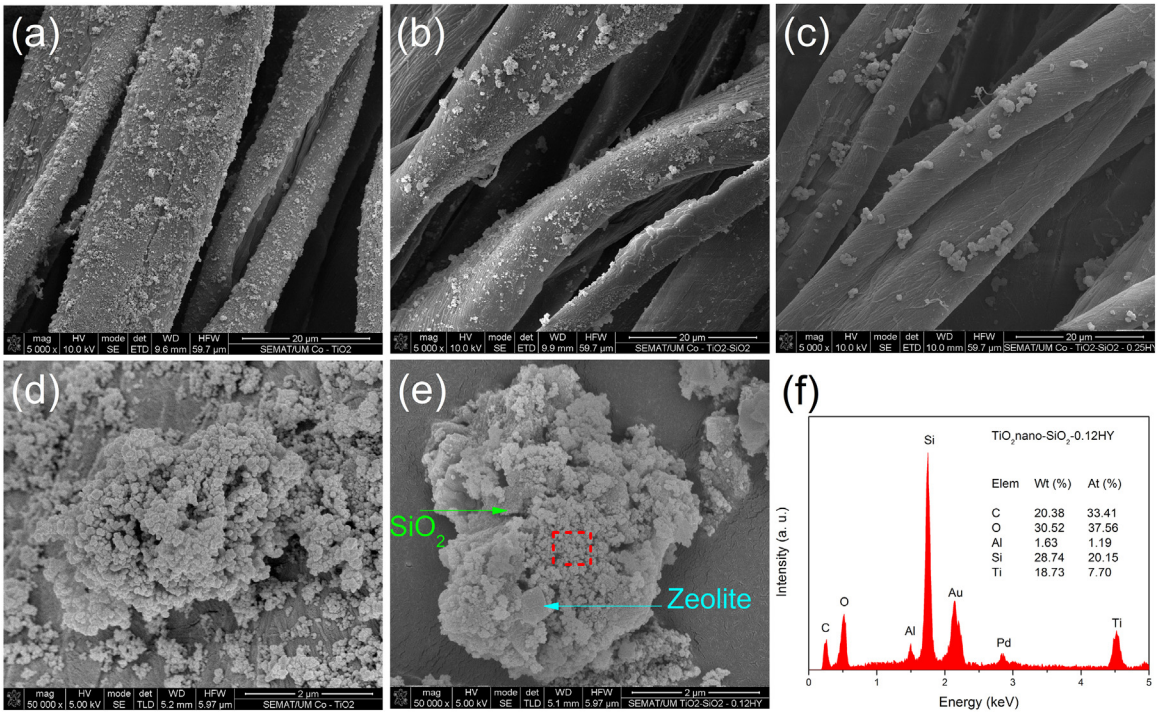

Fig. 2 – SEM micrographs of (a) TiO_2nano, (b) TiO_2nano-SiO_2 and (c) TiO_2nano-SiO_2-0.25HY deposited on cotton fibres at a magnification of 5000×, and morphology of (d) TiO_2 nanoparticles and (e) TiO_2nano-SiO_2-0.25HY nanocomposite at a magnification of 50,000×. (f) EDX analysis of TiO_2nano-SiO_2-0.25HY.

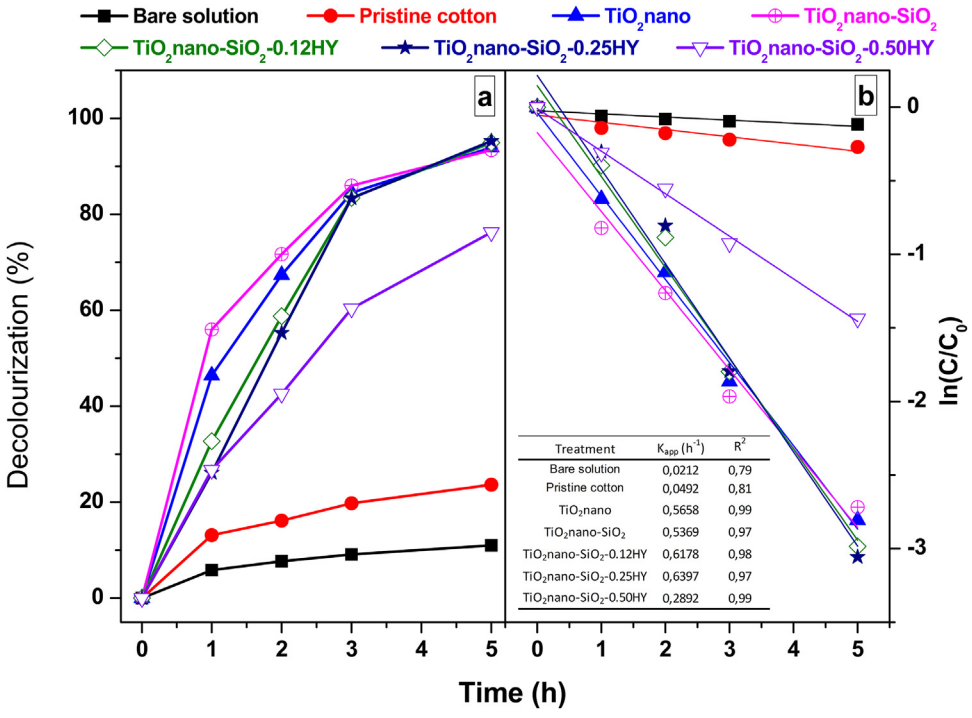

Fig. 3 – Decolourization of RhB solution under similar sunlight. Experimental conditions: 35 °C; $pH_{initial}$ = 5.9; [RhB] = 5.0 mg/L.

can be observed in Fig. 3(a), the decolourization of RhB bare solution was about 10% after having spent 5 h in light exposure conditions, demonstrating the photolysis occurrence of the RhB molecules. Meanwhile, within this same period of time, the RhB solution in the presence of pristine cotton experienced a decolourization equal to 26%. This increase can be probably related with two main factors: the presence of OH groups on the cellulose fibres and also due to O_2 trapped between the fibres. These species may form hydroxyl and superoxide radicals, respectively, contributing to improve the decolourization

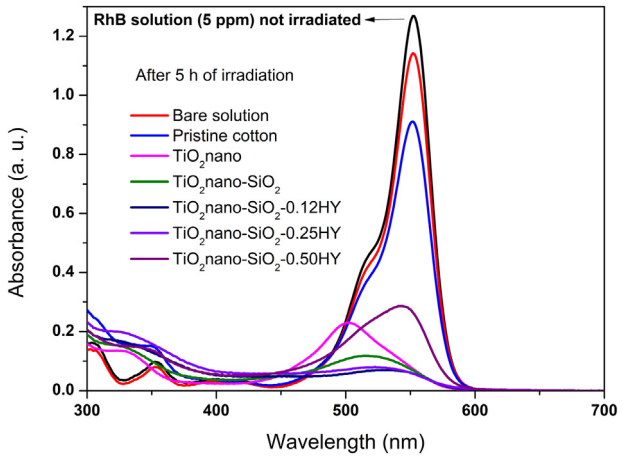

Fig. 4 – Degradation absorbance curves of RhB solution after 5 h of exposure to sunlight irradiation for the different nanocomposites compared to curves related with solutions treated with pristine cotton and without fabric (bare solution). Experimental conditions: 35 °C; $pH_{initial}$ = 5.9; [RhB] = 5.0 mg/L.

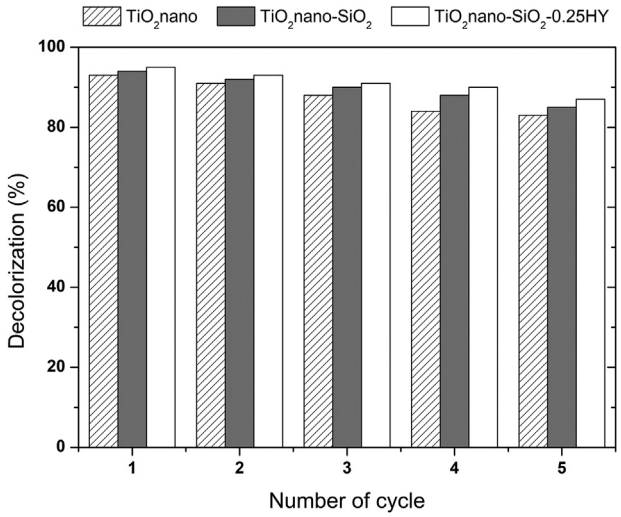

Fig. 5 – Stability tests of cotton fabrics coated with photocatalysts under simulated solar irradiation over a time period of 5 h. Experimental conditions: 35 °C; $pH_{initial}$ = 5.9; [RhB] = 5.0 mg/L.

of RhB solution when compared with the results obtained from its bare solution (that is, without the presence of any fabric).

On the other hand, the cotton fabrics coated with TiO_2nano, TiO_2nano-SiO_2, TiO_2nano-SiO_2-0.12HY and TiO_2nano-SiO_2-0.25HY induced the same solution decolourization (about 95%) after 5 h under simulated solar irradiation condition. According the SEM micrographs shown in Fig. 2, it can be observed that the cotton fibres are better coated by the photocatalysts that does not contain the HY zeolite. Even with less nanocomposites deposited on the cotton fibres, the decolourization of the RhB solution in the presence of the cotton substrate coated with TiO_2nano-SiO_2-(0.12 and 0.25)HY remained high after 5 h of exposure to light. However, from our experimental conditions, it was found that when a large amount of HY is present in the nanocomposites, the percentage decolourization of RhB solution decreases significantly, as can be observed from the curve shown in Fig. 3(a), which is represented by empty triangular symbols. Fig. 3(b) shows the variations in $\ln(C/C_0)$ with reaction time for the different treatments, in which the linear relationship between these variables indicates that RhB decolourization follows the pseudo-first-order kinetic model. It is also possible to observe that the decolourization rates for the treatments performed with the functionalized fabrics present the same order of magnitude, nevertheless the ones related to TiO_2nano-SiO_2-0.50 is substantially lower. These results suggest that smaller amounts of HY added to the composites have not a negative effect on the RhB degradation during the studied time interval.

Despite some of the samples showed the same decolourization over a period of 5 h, their absorbance spectra presented some peculiarities, as can be observed in Fig. 4. In fact, the solutions treated with cotton fabrics coated with the nanocomposites that hold 12% and 25% of HY zeolite material revealed a very similar optical behaviour. However, concerning the RhB solutions submitted to the treatment with photocatalysts without the zeolite material, it was observed that the absorbance of these aqueous solutions presented significant differences, mainly for the one that was treated with the sample that only contains TiO_2 nanoparticles.

As it is known, the shift of the maximum absorbance peak of the RhB towards lower wavelengths is related to the intermediates formed from the N-de-ethylation process [50]. Thus, the obtained UV-vis spectra for the RhB dye solutions treated with cotton fabrics coated with TiO_2nano, TiO_2nano-SiO_2 and TiO_2nano-SiO_2-HY photocatalysts suggest the presence of products that still preserve the chromophore structure of RhB dye. The relative amounts of these products will be discussed in detail in the next section.

In order to investigate the stability of self-cleaning fabrics, recycled photocatalytic degradation assays were performed for the cotton fabrics coated with TiO_2nano, TiO_2nano-SiO_2 and TiO_2nano-SiO_2-0.25HY photocatalysts (Fig. 5). From the analysis of Fig. 5 it can be stated that the RhB decolourization slightly decreased only after performing five consecutive cycles, denoting that these fabrics possess high recyclability and stability.

3.3. *Transformation products and photocatalytic mechanism*

The dye solutions subjected to different treatments were analyzed on the ion-trap mass spectrometer linked to the HPLC system (HPLC-MS) in positive ionization mode. Due to the lack of the appropriate standard compounds, these analyses enables to perform a comparative study concerning the N-de-ethylated intermediates present in different solutions, through the ratios of the corresponding peak areas. Fig. 6 depicts the chromatograms of the photodegraded solutions in the presence of cotton fabrics coated with TiO_2nano, TiO_2nano-SiO_2 and TiO_2nano-SiO_2-0.25HY photocatalysts.

The ion peaks (a–e) differ exactly by 28 mass units in sequence, which is consistent with the loss of the N-ethyl

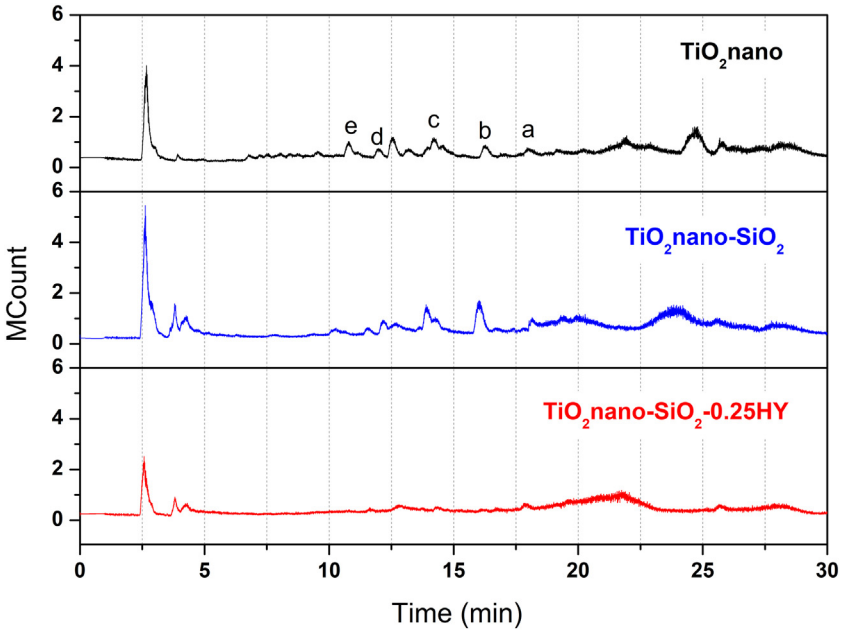

Fig. 6 – Total ion current chromatograms of the dye solutions after having been photocatalytically treated for 5 h with cotton fabrics coated with three different photocatalysts. The peaks (a–e) refer to the RhB ion and the intermediates that lost ethyl groups in sequence.

groups from the original RhB molecule. The areas of the peak "a" calculated for these three solutions were very similar denoting that the RhB concentration for these treated solutions is almost equal. On the other hand, the areas for the other peaks (b–e) showed significant differences, namely (i) the relative abundance of the full N-de-ethylated ion ($m/z = 331$, peak "e") for the solution, which was only treated with TiO_2 nanoparticles, is higher than that the one observed for the other two dye solutions, (ii) the concentration of the intermediates having a $m/z = 387$ (peak "c") and a $m/z = 415$ (peak "b") is higher for the solution treated with TiO_2nano-SiO_2 composite, and (iii) the bottom chromatogram, which correspond to the solution treatment carried out with the TiO_2nano-SiO_2-0.25HY composite, shows that all N-de-ethylated products of RhB exist in a lower concentration when compared with those observed for the other two solutions, showing that the presence of the HY zeolite material in the composite enhanced the RhB molecule degradation.

Since the aeration does not exist, it is expected that the superoxide radicals do not have much influence on the RhB degradation, being the photogenerated holes the main active species that participate in the photocatalytic mechanism. Based on this plausible supposition and from the results obtained above, the proposed mechanism for the RhB photocatalytic degradation, promoted by the cotton fabrics coated with the synthetized nanocomposites, can be the following: (i) electron–hole pairs are generated by the photocatalysts under UV and visible light irradiation; (ii) holes can be transferred to the water molecules producing hydroxyl radicals [51]; (iii) RhB molecules can also transfer electrons into the semiconductor CB by absorption of visible light at maximum of absorbance (553 nm) [52]; and (iv) acid sites present in the HY zeolite contribute for the degradation of the formed intermediate products.

3.4. *Cytotoxicity assay*

To assess the potential cytotoxic effect of the RhB before and after the photocatalytic treatment with fabrics functionalized with TiO_2nano, TiO_2nano-SiO_2 and TiO_2nano-SiO_2-0.25HY, human skin keratinocytes (NCTC 2544) cells were used as model of general cytotoxicity. Fig. 7 shows a decrease on cell viability with increasing concentrations of RhB for all the tested samples. However, this effect was more pronounced at the end of 48 h of exposition and it was only significant for the highest concentration (0.075 ppm) of RhB treated with TiO_2nano-SiO_2 and TiO_2nano-SiO_2-0.25HY when comparing with the negative control.

Despite the cytotoxic effect for the highest concentrations of RhB-species resulting from the TiO_2nano treatment, there was a slight increase on cell viability after 48 h of incubation for the lowest concentration of TiO_2 RhB-species. The RhB-species formed with this treatment seem to have a proliferative effect for the lowest tested concentration.

The effect of RhB (no treatment) on cell viability was more uniform for the tested concentrations when compared with the effect of the formed RhB-species, presenting cell viabilities ranging between $81 \pm 9\%$ and $93.8 \pm 0.9\%$.

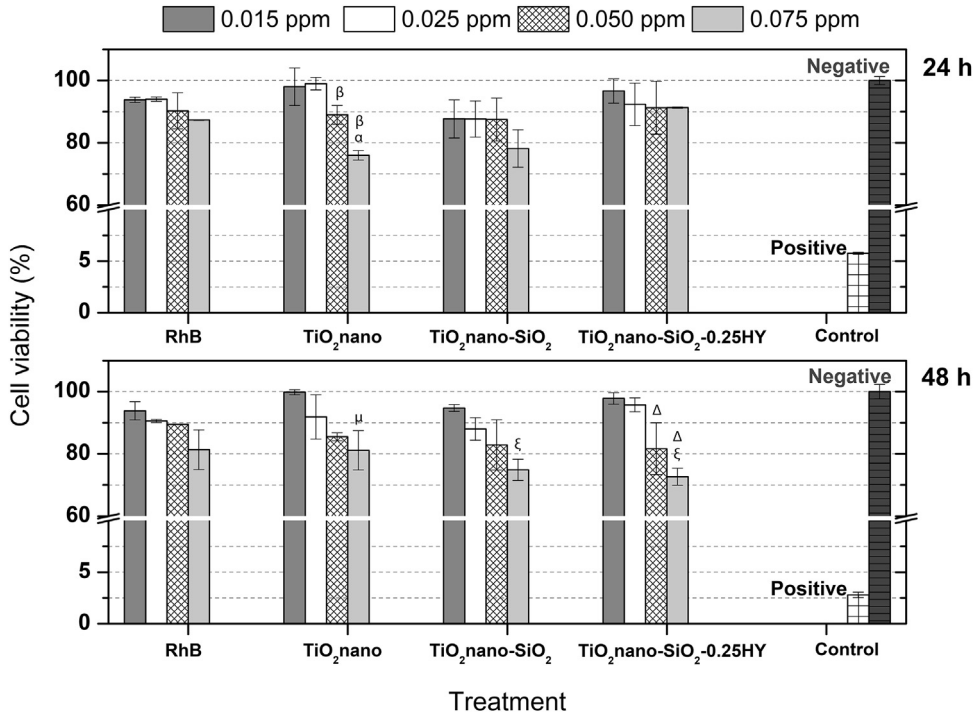

Fig. 7 – Relative viability of NCTC 2544 (human skin keratinocytes) evaluated with the MTT assay, after 24 and 48 h incubation in medium containing four concentrations (0.015, 0.025, 0.05 and 0.075 ppm) of RhB solutions obtained before and after treatment with textiles substrates functionalized with TiO_2nano, TiO_2nano-SiO_2 and TiO_2nano-SiO_2-0.25HY. Cells incubated with culture medium were used as negative control and cells incubated with 30% DMSO as positive control of cytotoxicity. Data were determined relative to the negative control (life). $\alpha P \leq 0.05$ when compared with negative control 24 h, $\xi P \leq 0.01$ when compared with negative control 48 h, $\Delta P \leq 0.01$ when compared with 0.075 ppm concentration of TiO_2nano-SiO_2-0.25HY treatment, $\beta P \leq 0.05$ when compared with 0.075 ppm concentration of TiO_2nano treatment 24 h, $\mu P \leq 0.05$ when compared with 0.075 ppm concentration of TiO_2nano treatment 48 h.

4. Conclusions

Photocatalysts based on TiO_2 nanoparticles, SiO_2 and different amounts of HY zeolite were successfully produced. XRD and FTIR analysis confirmed that the crystalline structure of the zeolite material did not change even after SiO_2-TiO_2nano loading. DRS reveal that the TiO_2 nanoparticles experienced N-doping during the syntheses, thus extending its light absorption range for longer wavelengths. The photocatalytic properties of cotton fabric functionalized with these nanocomposites were successfully confirmed via the RhB decolourization under simulated solar irradiation. It was observed that the presence of the HY zeolite in the nanocomposites does not change the RhB decolourization after 5 h of photocatalytic experiments but favoured the degradation of N-de-ethylated intermediates, excluding when a large amount of zeolite was used in the synthesis of the nanocomposites. It was observed that the effect of RhB dye and their photodegraded products on cell viability is dependent on time of incubation and RhB concentration. In general, the photodegradation of RhB dye solutions in the presence of cotton fabrics functionalized with TiO_2nano, TiO_2nano-SiO_2 and TiO_2nano-SiO_2-0.25HY resulted in the formation of species that were not much more cytotoxic than that of the original RhB solution, under the same tested concentrations and incubation times. Lastly, this work has shown that the photodegraded solutions by the fabrics coated with the synthesized composites presented a lower concentration of N-de-ethylated intermediates when compared with the ones that were only treated with cotton textiles coated by the TiO_2 semiconductor material. In this sense, it is possible to state that the use of fabrics coated with the synthesized composites do not present disadvantages for the tested cells relative to the initial RhB solution, for the same experimental conditions; in fact, some of the coated samples present environmental vantages, since it was verified a slight increase on cell viability.

Conflicts of interest

The authors declare no conflicts of interest.

Acknowledgements

Salmon Landi Jr. thanks the Capes from Brazil for supports his Doctoral Fellowship (Proc. no. 13346/13-0). The authors are also grateful to the financial support of the project "AIProcMat@N2020 – Advanced Industrial Processes and Materials for a Sustainable Northern Region of Portugal 2020", with the reference NORTE-01-0145-FEDER-000006 and the project BioTecNorte (operation NORTE-01-0145-FEDER-000004),

supported by Norte Portugal Regional Operational Programme (NORTE 2020), under the Portugal 2020 Partnership Agreement, through the European Regional Development Fund (ERDF). This work also has been funded by ERDF through COMPETE2020 – Programa Operacional Competitividade e Internacionalização (POCI), Project POCI-01-0145-FEDER-006984 – Associate Laboratory LSRE-LCM and by national funds through FCT – Fundação para a Ciência e a Tecnologia for project PTDC/AAGTEC/5269/2014 and Centre of Chemistry (UID/QUI/00686/2013 and UID/QUI/0686/2016). Artur Ribeiro thanks FCT for the SFRH\BPD\98388\2013 grant.

Appendix A. Supplementary data

Supplementary data associated with this article can be found, in the online version, at doi:10.1016/j.jmrt.2018.06.025.

REFERENCES

[1] Schneider J, Matsuoka M, Takeuchi M, Zhang J, Horiuchi Y, Anpo M, et al. Understanding TiO_2 photocatalysis: mechanisms and materials. Chem Rev 2014;114: 9919–86, http://dx.doi.org/10.1021/cr5001892.

[2] Gaya UI, Abdullah AH. Heterogeneous photocatalytic degradation of organic contaminants over titanium dioxide: a review of fundamentals, progress and problems. J Photochem Photobiol C Photochem Rev 2008;9:1–12, http://dx.doi.org/10.1016/j.jphotochemrev.2007.12.003.

[3] Perveen S, Farrukh MA. Ti0.85Sn0.15O2 nanocomposite: an efficient semiconductor photocatalyst for degradation of pesticides under solar light. J Mater Sci Mater Electron 2018;29:3219–30, http://dx.doi.org/10.1007/s10854-017-8257-8.

[4] He Y, Sutton NB, Rijnaarts HHH, Langenhoff AAM. Degradation of pharmaceuticals in wastewater using immobilized TiO_2 photocatalysis under simulated solar irradiation. Appl Catal B Environ 2016;182:132–41, http://dx.doi.org/10.1016/j.apcatb.2015.09.015.

[5] Natarajan S, Bajaj HC, Tayade RJ. Recent advances based on the synergetic effect of adsorption for removal of dyes from waste water using photocatalytic process. J Environ Sci (China) 2016:1–22, http://dx.doi.org/10.1016/j.jes.2017.03.011.

[6] Tahir M, Tahir B, Amin NS. Photocatalytic CO_2 reduction by CH_4 over montmorillonite modified TiO_2 nanocomposites in a continuous monolith photoreactor. Mater Res Bull 2015;63:13–23, http://dx.doi.org/10.1016/j.materresbull.2014.11.042.

[7] Cho JH, Eom Y, Jeon SH, Lee TG. A pilot-scale TiO_2 photocatalytic system for removing gas-phase elemental mercury at Hg-emitting facilities. J Ind Eng Chem 2013;19:144–9, http://dx.doi.org/10.1016/j.jiec.2012.07.016.

[8] Wang W, Huang G, Yu JC, Wong PK. Advances in photocatalytic disinfection of bacteria: development of photocatalysts and mechanisms. J Environ Sci (China) 2015;34:232–47, http://dx.doi.org/10.1016/j.jes.2015.05.003.

[9] Derikvandi H, Nezamzadeh-Ejhieh A. Synergistic effect of p–n heterojunction, supporting and zeolite nanoparticles in enhanced photocatalytic activity of NiO and SnO_2. J Colloid Interface Sci 2017;490:314–27, http://dx.doi.org/10.1016/j.jcis.2016.11.069.

[10] Khan SB, Hou M, Shuang S, Zhang Z. Morphological influence of TiO_2 nanostructures (nanozigzag, nanohelics and nanorod) on photocatalytic degradation of organic dyes. Appl Surf Sci 2017;400:184–93, http://dx.doi.org/10.1016/j.apsusc.2016.12.172.

[11] Han F, Kambala VSR, Srinivasan M, Rajarathnam D, Naidu R. Tailored titanium dioxide photocatalysts for the degradation of organic dyes in wastewater treatment: a review. Appl Catal A Gen 2009;359:25–40, http://dx.doi.org/10.1016/j.apcata.2009.02.043.

[12] Buthiyappan A, Aziz ARA, Wan Daud WMA. Recent advances and prospects of catalytic advanced oxidation process in treating textile effluents. Rev Chem Eng 2016;32:1–47, http://dx.doi.org/10.1515/revce-2015-0034.

[13] Sukriti, Sharma J, Chadha AS, Pruthi V, Anand P, Bhatia J, et al. Sequestration of dyes from artificially prepared textile effluent using RSM-CCD optimized hybrid backbone based adsorbent-kinetic and equilibrium studies. J Environ Manage 2017;190:176–87, http://dx.doi.org/10.1016/j.jenvman.2016.12.065.

[14] Nezamzadeh-Ejhieh A, Khorsandi M. Heterogeneous photodecolorization of Eriochrome Black T using Ni/P zeolite catalyst. Desalination 2010;262:79–85, http://dx.doi.org/10.1016/j.desal.2010.05.047.

[15] Khataee AR, Pons MN, Zahraa O. Photocatalytic degradation of three azo dyes using immobilized TiO_2 nanoparticles on glass plates activated by UV light irradiation: influence of dye molecular structure. J Hazard Mater 2009;168:451–7, http://dx.doi.org/10.1016/j.jhazmat.2009.02.052.

[16] Nezamzadeh-Ejhieh A, Khorsandi M. Photodecolorization of Eriochrome Black T using NiS-P zeolite as a heterogeneous catalyst. J Hazard Mater 2010;176:629–37, http://dx.doi.org/10.1016/j.jhazmat.2009.11.077.

[17] Park J. Visible and near infrared light active photocatalysis based on conjugated polymers. J Ind Eng Chem 2017;51:27–43, http://dx.doi.org/10.1016/j.jiec.2017.03.022.

[18] Farouk HU, Aziz ARA, Daud WMAW. TiO_2 catalyst deactivation in textile wastewater treatment: current challenges and future advances. J Ind Eng Chem 2016;33:11–21, http://dx.doi.org/10.1016/j.jiec.2015.10.022.

[19] Zabihi-Mobarakeh H, Nezamzadeh-Ejhieh A. Application of supported TiO_2 onto Iranian clinoptilolite nanoparticles in the photodegradation of mixture of aniline and 2,4-dinitroaniline aqueous solution. J Ind Eng Chem 2015;26:315–21, http://dx.doi.org/10.1016/j.jiec.2014.12.003.

[20] Guo X, Dai J, Zhang K, Wang X, Cui Z, Xiang J. Fabrication of N-doped TiO_2/activated carbon fiber composites with enhanced photocatalytic activity. Text Res J 2014;84:1891–900, http://dx.doi.org/10.1177/0040517514532159.

[21] Faraldos M, Bahamonde A. Environmental applications of titania-graphene photocatalysts. Catal Today 2017;285:13–28, http://dx.doi.org/10.1016/j.cattod.2017.01.029.

[22] Cetinkaya T, Neuwirthová L, Kutláková K, Tomásek V, Akbulut H. Synthesis of nanostructured TiO_2/SiO_2 as an effective photocatalyst for degradation of acid orange. Appl Surf Sci 2013;279:384–90, http://dx.doi.org/10.1016/j.apsusc.2013.04.121.

[23] Nagarjuna R, Roy S, Ganesan R. Polymerizable sol–gel precursor mediated synthesis of TiO_2 supported zeolite-4A and its photodegradation of methylene blue. Micropor Mesopor Mater 2015;211:1–8, http://dx.doi.org/10.1016/j.micromeso.2015.02.044.

[24] Guesh K, Márquez-Álvarez C, Chebude Y, Díaz I. Enhanced photocatalytic activity of supported TiO_2 by selective surface modification of zeolite y. Appl Surf Sci 2016;378:473–8, http://dx.doi.org/10.1016/j.apsusc.2016.04.029.

[25] Guesh K, Mayoral Á, Márquez-Álvarez C, Chebude Y, Díaz I. Enhanced photocatalytic activity of TiO_2 supported on zeolites tested in real wastewaters from the textile industry

of Ethiopia. Micropor Mesopor Mater 2016;225:88–97, http://dx.doi.org/10.1016/j.micromeso.2015.12.001.
[26] Nezamzadeh-Ejhieh A, Bahrami M. Investigation of the photocatalytic activity of supported ZnO–TiO_2 on clinoptilolite nano-particles towards photodegradation of wastewater-contained phenol. Desalin Water Treat 2015;55:1096–104, http://dx.doi.org/10.1080/19443994.2014.922443.
[27] Mohammadyari P, Nezamzadeh-Ejhieh A. RSC advances supporting of mixed ZnS–NiS semiconductors onto clinoptilolite nano-particles to improve its activity in photodegradation of 2-nitrotoluene. RSC Adv 2015;5:75300–10, http://dx.doi.org/10.1039/C5RA12608H.
[28] Nezamzadeh-Ejhieh A, Karimi-shamsabadi M. Decolorization of a binary azo dyes mixture using CuO incorporated nanozeolite-X as a heterogeneous catalyst and solar irradiation. Chem Eng J 2013;228:631–41, http://dx.doi.org/10.1016/j.cej.2013.05.035.
[29] Nezamzadeh-Ejhieh A, Shahriari E. Photocatalytic decolorization of methyl green using Fe(II)-o-phenanthroline as supported onto zeolite Y. J Ind Eng Chem 2014;20:2719–26, http://dx.doi.org/10.1016/j.jiec.2013.10.060.
[30] Landi S, Carneiro J, Ferdov S, Fonseca AM, Neves IC, Ferreira M, et al. Photocatalytic degradation of Rhodamine B dye by cotton textile coated with SiO_2-TiO_2 and SiO_2-TiO_2-HY composites. J Photochem Photobiol A Chem 2017;346:60–9, http://dx.doi.org/10.1016/j.jphotochem.2017.05.047.
[31] Silvestri S, Hennemann B, Zanatta N, Foletto EL. Photocatalytic efficiency of TiO_2 supported on Raw Red Clay Disks to Discolour Reactive Red 141. Water Air Soil Pollut 2018;229:1–12.
[32] Fan Y, Zhou J, Zhang J, Lou Y, Huang Z, Ye Y, et al. Photocatalysis and self-cleaning from g-C3N4 coated cotton fabrics under sunlight irradiation. Chem Phys Lett 2018;699:146–54, http://dx.doi.org/10.1016/j.cplett.2018.03.048.
[33] El-Naggar ME, Hassabo AG, Mohamed AL, Shaheen TI. Surface modification of SiO_2 coated ZnO nanoparticles for multifunctional cotton fabrics. J Colloid Interface Sci 2017;498:413–22, http://dx.doi.org/10.1016/j.jcis.2017.03.080.
[34] El-Naggar ME, Shaheen TI, Zaghloul S, El-Rafie MH, Hebeish A. Antibacterial activities and UV protection of the in situ synthesized titanium oxide nanoparticles on cotton fabrics. Ind Eng Chem Res 2016;55:2661–8, http://dx.doi.org/10.1021/acs.iecr.5b04315.
[35] Mohamed AL, El-Naggar ME, Shaheen TI, Hassabo AG. Laminating of chemically modified silan based nanosols for advanced functionalization of cotton textiles. Int J Biol Macromol 2017;95:429–37, http://dx.doi.org/10.1016/j.ijbiomac.2016.10.082.
[36] Katouei Zadeh E, Zebarjad SM, Janghorban K. Synthesis and enhanced visible-light activity of N-doped TiO_2 nano-additives applied over cotton textiles. J Mater Res Technol 2017:1–8, http://dx.doi.org/10.1016/j.jmrt.2017.05.011.
[37] Jain R, Mathur M, Sikarwar S, Mittal A. Removal of the hazardous dye rhodamine B through photocatalytic and adsorption treatments. J Environ Manage 2007;85:956–64, http://dx.doi.org/10.1016/j.jenvman.2006.11.002.
[38] Xu B, Ding J, Feng L, Ding Y, Ge F, Cai Z. Self-cleaning cotton fabrics via combination of photocatalytic TiO_2 and superhydrophobic SiO_2. Surf Coat Technol 2015;262:70–6, http://dx.doi.org/10.1016/j.surfcoat.2014.12.017.
[39] Zhang DR, Liu HL, Han SY, Piao WX. Synthesis of Sc and V-doped TiO_2 nanoparticles and photodegradation of rhodamine-B. J Ind Eng Chem 2013;19:1838–44, http://dx.doi.org/10.1016/j.jiec.2013.02.029.
[40] Ribeiro A, Matamá T, Cruz CF, Gomes AC, Cavaco-Paulo AM. Potential of human cD-crystallin for hair damage repair: insights into the mechanical properties and biocompatibility. Int J Cosmet Sci 2013;35:458–66, http://dx.doi.org/10.1111/ics.12065.
[41] Baerlocher C, McCusker L, Olson D. Atlas of zeolite framework types. sixth ed. Elsevier; 2007.
[42] Freitas CMAS, Soares OSGP, Órfão JJM, Fonseca AM, Pereira MFR, Neves IC. Highly efficient reduction of bromate to bromide over mono and bimetallic ZSM5 catalysts. Green Chem 2015;17:4247–54, http://dx.doi.org/10.1039/C5GC00777A.
[43] Bahrami M, Nezamzadeh-Ejhieh A. Effect of supporting and hybridizing of FeO and ZnO semiconductors onto an Iranian clinoptilolite nano-particles and the effect of ZnO/FeO ratio in the solar photodegradation of fish ponds waste water. Mater Sci Semicond Process 2014;27:833–40, http://dx.doi.org/10.1016/j.mssp.2014.08.030.
[44] Kemdeo SM, Sapkal VS, Chaudhari GN. TiO_2-SiO_2 mixed oxide supported MoO3 catalyst: physicochemical characterization and activities in nitration of phenol. J Mol Catal A Chem 2010;323:70–7, http://dx.doi.org/10.1016/j.molcata.2010.03.017.
[45] Esmaili-Hafshejani J, Nezamzadeh-Ejhieh A. Increased photocatalytic activity of Zn(II)/Cu(II) oxides and sulfides by coupling and supporting them onto clinoptilolite nanoparticles in the degradation of benzophenone aqueous solution. J Hazard Mater 2016;316:194–203, http://dx.doi.org/10.1016/j.jhazmat.2016.05.006.
[46] Azimi S, Nezamzadeh-Ejhieh A. Enhanced activity of clinoptilolite-supported hybridized PbS-CdS semiconductors for the photocatalytic degradation of a mixture of tetracycline and cephalexin aqueous solution. J Mol Catal A Chem 2015;408:152–60, http://dx.doi.org/10.1016/j.molcata.2015.07.017.
[47] Reza M, Khaki D, Saleh M, Aziz ARA, Mohd W, Wan A. Application of doped photocatalysts for organic pollutant degradation – a review. J Environ Manage 2017;198:78–94, http://dx.doi.org/10.1016/j.jenvman.2017.04.099.
[48] Kumar SG, Devi LG. Review on modified TiO_2 photocatalysis under UV/visible light: selected results and related mechanisms on interfacial charge carrier transfer dynamics. J Phys Chem A 2011;115:13211–41.
[49] Sadiq MMJ, Nesaraj AS. Reflux condensation synthesis and characterization of Co_3O_4 nanoparticles for photocatalytic applications. Iran J Catal 2014;4:219–26.
[50] Zhao J, Wu T, Wu K, Oikawa K, Hidaka H, Serpone N. Photoassisted degradation of dye pollutants. V. Self-photosensitized oxidative transformation of Rhodamine B under visible light irradiation in aqueous TiO_2 dispersions. J Phys Chem B 1998;102:5845–51, http://dx.doi.org/10.1021/jp980922c.
[51] Merouani S, Hamdaoui O, Saoudi F, Chiha M. Sonochemical degradation of Rhodamine B in aqueous phase: effects of additives. Chem Eng J 2010;158:550–7, http://dx.doi.org/10.1016/j.cej.2010.01.048.
[52] Landi S, Carneiro JO, Fernandes F, Parpot P, Molina J, Cases F, et al. Functionalization of cotton by RGO/TiO_2 to enhance photodegradation of Rhodamine B under simulated solar irradiation. Water Air Soil Pollut 2017;228:335, http://dx.doi.org/10.1007/s11270-017-3533-z.